THE JOURNAL OF PHYSICAL CHEMISTRY Letters

Letter

pubs.acs.org/JPCL

Surface Effect of Alumina on the First Electronic Transition of Liquid Water Studied by Far-Ultraviolet Spectroscopy

Takeyoshi Goto,*[,†] Akifumi Ikehata,[‡] Yusuke Morisawa,[§] and Yukihiro Ozaki[†]

[†]Department of Chemistry, School of Science and Technology, Kwansei Gakuin University, Sanda, Hyogo 669-1337, Japan

[‡]National Food Research Institute, National Agriculture and Food Research Organization (NARO), Tsukuba, Ibaraki 305-8642, Japan

[§]Department of Chemistry, School of Science and Engineering, Kinki University, Higashi-Osaka, Osaka 577-8502, Japan

Supporting Information

ABSTRACT: The first electronic transition ($\tilde{A} \leftarrow \tilde{X}$) of liquid water ($H_2O$ and D_2O) on an α-alumina substrate was studied using variable angle attenuated total reflection far-ultraviolet (VA-ATR-FUV) spectroscopy in the wavelength region 140−180 nm (8.86−6.89 eV). A variation in the penetration depth of the evanescent wave of a probe light (25−19 nm) directly determined individual FUV spectra associated with bulk water (distance from the alumina surface >2 nm) and interfacial water (<2 nm). We found that the $\tilde{A} \leftarrow \tilde{X}$ band of the interfacial water was markedly blue-shifted and red-tailed relative to the bulk water. The electronic state difference of the interfacial water from the bulk water mainly arose from the hydrogen-bond structure and energy affected by the alumina surface.

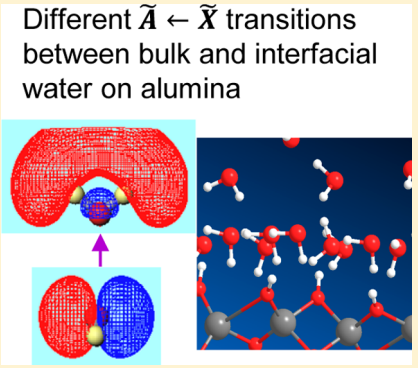

Although ultraviolet (UV) photoabsorption of liquid water is a fundamental photochemical process in nature, the original reports on the spectral measurement of the first electronic transition ($\tilde{A} \leftarrow \tilde{X}$) of liquid water were conducted less than half a century ago.[1−3] The most challenging part of investigating the $\tilde{A} \leftarrow \tilde{X}$ transition of liquid water is that the absorption coefficient (α) steeply rises by 7 orders of magnitude in far-UV (FUV) region ($\sim 2 \times 10^5$ cm^{-1} at 8.3 eV) in contrast to its high optical transparency in near-UV and visible light regions.[1,3−6] Because of the high surface tension of pure water, it is impractical to measure the transmission spectrum of liquid water.[2,3] The FUV spectrum of liquid water describing the entire $\tilde{A} \leftarrow \tilde{X}$ band was originally reported with an external reflection method by Painter in 1968.[1] Since then, the spectral measurement of the entire $\tilde{A} \leftarrow \tilde{X}$ band has been rarely reported due to the experimental difficulty, despite intensive progress in the theoretical aspects.[7,8] In order to measure the FUV spectra of liquid water more practically, we developed an attenuated total reflection (ATR)-type FUV spectrophotometer employing a single-crystal alumina prism.[4,9] The accumulation of spectral measurements unveil how the electronic states of pure water and aqueous solutions are associated with the hydrogen-bond (H-bond) energy from the temperature difference spectra of pure water and the spectra of the various electrolyte solutions.[5,6,10]

However, the measured FUV spectrum of liquid water with either a transmission or reflection method does not represent the electronic transition of bulk liquid water, because the extremely short path length causes a strong surface effect of the solid substrate on the liquid structure of water molecules. The X-ray,[11] sum-frequency vibrational (SFV),[12] and infrared (IR)[13,14] spectroscopic studies with molecular dynamics (MD) simulations[15] show that the partially charged aluminol groups on the surface perturb the local density of liquid water and induce the formation of highly dense hydration layers extended up to ∼2 nm from the surface. Consequently, the physical properties of the interfacial water (density, viscosity, and dielectric constant) are distinctively different from those of the bulk water.[16−18] Hence, it is expected that the $\tilde{A} \leftarrow \tilde{X}$ transitions of the interfacial water is markedly different from the bulk water.

Herein, we revealed the $\tilde{A} \leftarrow \tilde{X}$ transition of liquid water (H_2O and D_2O) on an alumina surface by measuring the ATR-FUV spectrum of liquid water with various incident angles of a probe light (θ). The individual spectra of bulk and interfacial water were determined by linearly decomposing the measured variable angle (VA) spectra based on the spectral changes with the penetration depth of the evanescent wave of the probe light (d_p) from the alumina surface.[19]

The broad $\tilde{A} \leftarrow \tilde{X}$ bands of liquid water were observed around 8.45 eV for H_2O and 8.53 eV for D_2O (Figure 1). As θ increased from 58.4° to 71.8°, the $\tilde{A} \leftarrow \tilde{X}$ band maxima (λ_{max}) were blue-shifted from 8.41 to 8.48 eV for H_2O and 8.49 to 8.57 eV for D_2O, the α values increased from 2.01×10^5 cm^{-1} to 2.39×10^5 cm^{-1} for H_2O and 1.99×10^5 cm^{-1} to 2.41×10^5 cm^{-1} for D_2O, and the half-width at half-maximum (HWHM) on the longer-wavelength side increased from 0.598 to 0.630 eV

Received: January 28, 2015
Accepted: March 5, 2015
Published: March 5, 2015

DOI: 10.1021/acs.jpclett.5b00190
J. Phys. Chem. Lett. 2015, 6, 1022−1026

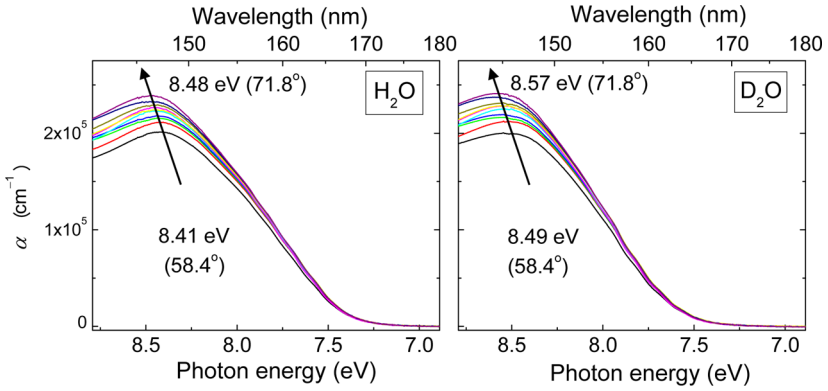

Figure 1. Far-ultraviolet absorption spectra of H_2O (left) and D_2O (right) with various incident angles shown in parentheses.

Table 1. $\tilde{A} \leftarrow \tilde{X}$ Band Parameters of Liquid Water in Bulk and Interfacial Phases and Ice States (Amorphous and Ih); Transition Energy at Band Maximum (λ_{max}/eV), Absorption Coefficient ($\alpha/10^5$ cm^{-1}), Molar Absorption Coefficient [$\varepsilon = (\alpha/c\ln 10)/10^3$ L mol^{-1}cm^{-1}; c, concentration (molL^{-1})], and Half-Width at Half-Maximum (HWHM/eV)[a]

	H_2O					D_2O			
	measured value	bulk	interface	ice (amorphous)	ice (Ih)	measured value	bulk	interface	ice
λ_{max}	8.41−8.48	8.37	8.63	8.64	8.65	8.49−8.57	8.43	8.68	8.75*
α	2.01−2.39	1.81	6.89	2.72	3.59	1.99−2.41	1.77	7.12	
ε	1.58−1.87	1.42				1.58−1.90	1.40		
HWHM	0.598−0.630	0.600	0.623	0.560	0.476	0.538−0.585	0.519	0.562	

[a]Those of ice states were obtained from refs 20 and 21. *λ_{max} was obtained from the raw reflection spectrum.

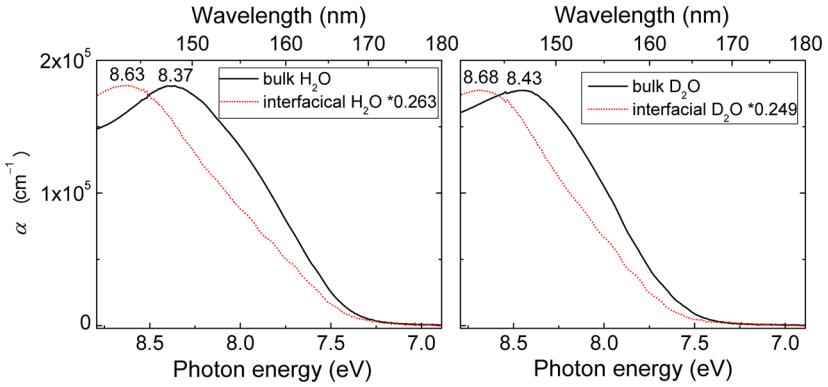

Figure 2. Resolved far-ultraviolet spectra of the bulk (d_p > 2 nm) and interfacial (<2 nm) water for H_2O (left) and D_2O (right); d_p, penetration depth of evanescent wave of probe light.

and 0.538 to 0.585 eV for D_2O. Because the θ variation corresponds to a change in the d_p length, the observed spectral changes were ascribed to the extent of the interfacial water contribution to the measured spectra. Therefore, the observed spectral features as increasing θ (shortening d_p); blue-shift, increasing absorptivity, and broadening bandwidth, reflected the electronic nature of the interfacial water. The measured $\tilde{A} \leftarrow \tilde{X}$ band parameters (λ_{max}, α, and HWHM) of H_2O and D_2O at the smallest and largest θ are listed in Table 1.

The VA spectral analysis revealed that the $\tilde{A} \leftarrow \tilde{X}$ transitions of the bulk water (d_p > 2 nm) and the interfacial water (<2 nm) were quite different (Figure 2). The optimum spectra of the bulk and interfacial phases were calculated with the alternating least-squares (ALS) method by assuming that the thickness of the interfacial water layer on the alumina surface is ∼2 nm. From the X-ray[11] and MD[15] studies of the water−alumina interface, the density of water molecule fluctuates from the alumina surface until ∼1.5 nm. So, ALS calculations were tried with the initial value of the interfacial thickness (l_{ini}) from 0.5 to 3 nm. Then the ALS result from l_{ini} = 2 nm was selected, because the fitting error was the smallest. The maximum percent relative uncertainty of the fitting result was about 10%. The details of the VA spectral analysis are described in the Supporting Information (SI). The λ_{max} value of the interfacial water was larger than that of the bulk water by 0.26 eV for H_2O and 0.25 eV for D_2O, the α value of the interfacial water was 3.8 times larger for H_2O and 4.0 times for D_2O, and the red-tailing of the $\tilde{A} \leftarrow \tilde{X}$ band on the longer-wavelength side was observed only for the interfacial water. The $\tilde{A} \leftarrow \tilde{X}$ band parameters of the bulk and interfacial water are compared in Table 1 with those of the solid states (hexagonal crystal (Ih) and amorphous) from refs 20 and 21. SI Figure S1 shows the imaginary part of the refractive index (k) of the bulk water compared with the literature values of liquid water from refs 1 and 3.

DOI: 10.1021/acs.jpclett.5b00190
J. Phys. Chem. Lett. 2015, 6, 1022−1026

The higher $\tilde{A} \leftarrow \tilde{X}$ transition energy of the interfacial water relative to the bulk water was associated with the stronger H-bond network of the interfacial water. Figure 3 shows the

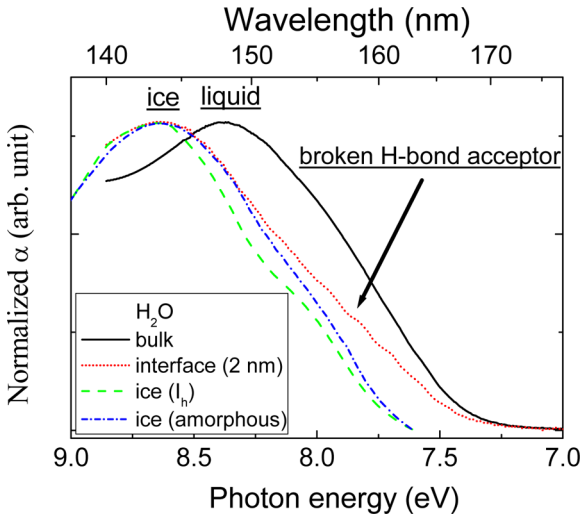

Figure 3. Normalized $\tilde{A} \leftarrow \tilde{X}$ bands of bulk and interfacial H_2O in the liquid state determined by the present experiment and those of Ih and amorphous ice states obtained from ref 20.

normalized $\tilde{A} \leftarrow \tilde{X}$ bands of liquid H_2O in the bulk and interfacial phases and those of the solid H_2O in the Ih and amorphous phases.[20] The band maximum position of the interfacial water was much closer to those of the solid states than that of the bulk water. The $\tilde{A} \leftarrow \tilde{X}$ transition energy of water is blue-shifted as the H-bond network is denser and more structured (λ_{max}: ~7.4 eV for vapor state,[22,23] ~8.3 eV for liquid,[1−7] and ~8.7 eV for solid[20,21]) because of the excitation of the nonbonding electrons on the oxygen atom, which also acts as an H-bond acceptor.[24] The $\tilde{A} \leftarrow \tilde{X}$ band of liquid H_2O is blue-shifted from 8.26 to 8.40 eV, and its absorptivity increases by 12% under constant θ (60°), as the temperature decreases from 70 to 10 °C.[5] From an electronic state calculation of water pentamer clusters, the blue-shift of the $\tilde{A} \leftarrow \tilde{X}$ band of the water cluster relative to the water monomer arises from the electronic excitation of the H-bond making electrons destabilize the excited states of the water molecules.[7]

However, the interfacial water spectrum was not the same as those of the solid states. The α value of the interfacial H_2O was 2.5 and 1.9 times larger than those of amorphous and Ih ice states, respectively (Table 1). Also, the red-tailing of the $\tilde{A} \leftarrow \tilde{X}$ band does not appear in the ice state spectra (Figure 3). The FUV spectroscopic studies of water ice[7,8] and the theoretical studies of water clusters[24,25] suggest that the red-tailing of the $\tilde{A} \leftarrow \tilde{X}$ band is peculiarly ascribed to the weakly H-bonded water molecules. The electronic state calculation of water pentamer clusters shows that the $\tilde{A} \leftarrow \tilde{X}$ transition energies of the nonbonding electrons in a fully H-bond acceptor water molecule located at the cluster center are higher than those in the monomer by 0.7 eV, while those in the broken H-bond acceptor ones located on the cluster surface are lower by 0.2 eV.[7] Also, it is noteworthy to support the ascription of the red-tailing that the linear combination of the bulk water and Ih ice spectra did not reproduce the red-tailing of the $\tilde{A} \leftarrow \tilde{X}$ band. Consequently, the interfacial water spectrum reflected a denser and more structured H-bond network accompanied by broken H-bond acceptors relative to the bulk water formed 2 nm below from the alumina surface.

The observed spectral features of the interfacial water relative to the bulk water; the blue-shift and the red-tailing of the $\tilde{A} \leftarrow \tilde{X}$ bands were associated with the forced H-bond structure and energy by the alumina surface. A two-dimensional bilayer model of the alumina−water interface was proposed to reconcile not well-defined point of zero charge (pzc) of the alumina surface.[26] The first water layer on the alumina forms a tetrahedrally coordinated H-bond structure with the other water molecules in the layer and with the hydroxyl groups of the alumina. The partial charges localized on the $Al_2OH_2^{+0.5}$ and $AlOH^{-0.5}$ groups weakly induce the local ordering of the first layer molecules in the slightly acidic pH region.[12] This dense ice-like water layer accompanies the higher $\tilde{A} \leftarrow \tilde{X}$ transition energies of the interfacial water by ~0.25 eV and the lower OH vibrational band[12−14] by ~100 cm^{-1} relative to the bulk water. Because the strong H-bond structure in the first layer makes fewer dangling OH bonds to the second layer, the first layer might be hydrophobic to the subsequent layers.[26−28] The red-tailed bands of the $\tilde{A} \leftarrow \tilde{X}$ transition in the interfacial spectra were ascribed to the dangling OH bonds or broken H-bond acceptors of the water molecules existing near the first layer surface and to liquid-like structure in the subsequent layers. Therefore, the proposed H-bond structure model of the alumina−water interface could explain that the electronic structure differences between the bulk and interfacial water mainly arose from the H-bond energy difference between the ground and excited states, and this is in line with the electronic state calculation of a small water cluster[29] and the temperature-different FUV spectrum of liquid water.[5]

The examination of deuterium effects on the bulk and interfacial FUV spectra elucidated the electronic nature of the $\tilde{A} \leftarrow \tilde{X}$ transition of liquid water. The lower ground state electronic energy of D_2O relative to H_2O mainly caused the higher $\tilde{A} \leftarrow \tilde{X}$ transition energy of D_2O. The $\tilde{A} \leftarrow \tilde{X}$ transition energy differences between H_2O and D_2O (0.057 and 0.047 eV for the bulk and interfacial phases, respectively) were equivalent to the zero-point vibrational energy (ZPVE) difference between the O−H and O−D stretching modes ($ZPVE_{O-H} - ZPVE_{O-D}$ = 0.053 eV). The $\tilde{A} \leftarrow \tilde{X}$ bands of D_2O were contracted relative to H_2O, because D_2O molecules form a stronger and more well-defined H-bond network than H_2O molecules due to the smaller molecular size and lower ZPVE.[30,31] The HWHM value of the $\tilde{A} \leftarrow \tilde{X}$ band of D_2O was smaller by 13.5% for the bulk phase and 9.8% for the interfacial phase. The higher absorptivity of the interfacial D_2O band indicated that the H-bond network of the interfacial D_2O molecules was more compressed on the alumina surface than that of H_2O. The α value ratio of the interfacial phase to the bulk phase was 5.4% larger for D_2O than H_2O. Consequently, the concentration ratio of the interfacial phase to the bulk phase was also larger for D_2O. This is consistent with the result that the more well-defined tetrahedral and open structure of the H-bond network of D_2O makes liquid D_2O ~4% more compressible than liquid H_2O at room temperature.[32,33]

We can conclude that the VA-ATR-FUV spectral analysis of liquid water on the alumina substrate revealed the pure $\tilde{A} \leftarrow \tilde{X}$ transition spectra of the bulk and interfacial water. The alumina surface strongly affected the electronic state of liquid water. The interfacial water spectra exhibited the blue-shift and the red-tailing of the $\tilde{A} \leftarrow \tilde{X}$ band relative to the bulk water. These spectral differences of the interfacial water were derived from

DOI: 10.1021/acs.jpclett.5b00190
J. Phys. Chem. Lett. 2015, 6, 1022−1026

the H-bond structure and energy affected by the alumina surface. The partially charged hydroxyl groups on the alumina surface formed a strong H-bond layer in the first layer, and its hydrophobicity caused the broken H-bond acceptors and liquid-like H-bonds in the subsequent layers. It is also noteworthy that the $\tilde{A} \leftarrow \tilde{X}$ transition of the bulk liquid water was revealed by exclusion of the surface effect. The deuterium effects on the electronic spectra of liquid water corresponded with the stronger H-bond interaction of D_2O, which made its interfacial structure more compressed than that of H_2O.

EXPERIMENTAL METHODS

Pure water was prepared using deionized water from a Milli-Q system (water resistivity 18.2 MΩ cm, TOC 3 ppb, Millipore Corp.). D_2O (99.95 atom %) was purchased from Acros Organic (USA) and used as received. The liquid H_2O and D_2O were slightly acidic (pH = ∼6) due to dissolved CO_2. A highly polished α-Al_2O_3 crystal (R-plane) prism (Kyocera Corp., Japan) was prepared, because the surface roughness of a prism could affect the H-bond structure of the interfacial water. The average roughness (R_a) of the prism surface is about 5 Å measured with atomic force microscopy.

VA-ATR-FUV spectra were measured at 25.0 ± 1.0 °C with a spectrophotometer designed by our group,[4,9] which comprised a D_2 lamp, a monochromator (KV-200, Bunkoh-Keiki Co. Ltd.), the α-Al_2O_3 prism, and a photomultiplier tube equipped with a fused silica plate coated with a sodium salicylate film. The probe light path was continuously purged with N_2 gas to reduce the absorption of FUV light by atmospheric oxygen and water vapor. θ varied from 58.4° to 71.8°. The ATR absorbance is defined as $-\log(I/I_0)$, where I is the reflected light intensity for a sample solution and I_0 is that for a reference (N_2). Because of the difficulty to prepare a fully dry alumina prism surface for the reference measurements, the alumina prism, set on the ATR position, was washed with pure ethanol and dried with high-purity N_2 gas blow for ∼10 min. Then, the sample compartment was sealed, and the reference spectra were measured. The complex refractive indices of liquid water were calculated with a Kramers−Kronig transformation from the measured ATR-FUV spectra as shown in the SI.

ASSOCIATED CONTENT

Supporting Information

Details of Kramer−Kronig transformation of the measured ATR spectra and the VA spectral analysis, Figure S1, which shows the imaginary part of the refractive index of the bulk water with the literature values from the refs 1 and 3, and Table S1, which shows d_e and d_p with θ. This material is available free of charge via the Internet at http://pubs.acs.org/.

AUTHOR INFORMATION

Notes

The authors declare no competing financial interest.

ACKNOWLEDGMENTS

This work is supported by the System Development Program for Advanced Measurement and Analysis of the Japan Science and Technology Agency.

REFERENCES

(1) Division, H. P.; Ridge, O.; Painter, L. R. Optical Measurements of Liquid Water in the Vacuum Ultraviolet. *J. Chem. Phys.* **1969**, *51*, 243−251.
(2) Verrall, R. E. Vacuum-Ultraviolet Study of Liquid H_2O and D_2O. *J. Chem. Phys.* **1969**, *50*, 2746−2750.
(3) Sowers, B. L. Optical Absorption of Liquid Water in the Vacuum Ultraviolet. *J. Chem. Phys.* **1972**, *57*, 583−584.
(4) Ozaki, Y.; Morisawa, Y.; Ikehata, A.; Higashi, N. Far-Ultraviolet Spectroscopy in the Solid and Liquid States: A Review. *Appl. Spectrosc.* **2012**, *66*, 1−25.
(5) Ikehata, A.; Higashi, N.; Ozaki, Y. Direct Observation of the Absorption Bands of the First Electronic Transition in Liquid H_2O and D_2O by Attenuated Total Reflectance Far-UV Spectroscopy. *J. Chem. Phys.* **2008**, *129*, 234510:1−5.
(6) Goto, T.; Ikehata, A.; Morisawa, Y.; Ozaki, Y. Electronic Transitions of Protonated and Deprotonated Amino Acids in Aqueous Solution in the Region 145−300 nm Studied by Attenuated Total Reflection Far-Ultraviolet Spectroscopy. *J. Phys. Chem. A* **2013**, *117*, 2517−2528.
(7) Cabral do Couto, P.; Chipman, D. M. Insights into the Ultraviolet Spectrum of Liquid Water from Model Calculations: The Different Roles of Donor and Acceptor Hydrogen Bonds in Water Pentamers. *J. Chem. Phys.* **2012**, *137*, 184301:1−14.
(8) Oncák, M.; Slavícek, P.; Poterya, V.; Fárník, M.; Buck, U. Emergence of Charge-Transfer-to-Solvent Band in the Absorption Spectra of Hydrogen Halides on Ice Nanoparticles: Spectroscopic Evidence for Acidic Dissociation. *J. Phys. Chem. A* **2008**, *112*, 5344−5353.
(9) Higashi, N.; Ikehata, A.; Ozaki, Y. An Attenuated Total Reflectance Far-UV Spectrometer. *Rev. Sci. Instrum.* **2007**, *78*, 103107:1−5.
(10) Goto, T.; Ikehata, A.; Morisawa, Y.; Higashi, N.; Ozaki, Y. The Effect of Metal Cations on the Nature of the First Electronic Transition of Liquid Water as Studied by Attenuated Total Reflection Far-Ultraviolet Spectroscopy. *Phys. Chem. Chem. Phys.* **2012**, *14*, 8097−8104.
(11) Catalano, J. G.; Park, C.; Zhang, Z.; Fenter, P. Termination and Water Adsorption at the α-Al_2O_3 (012)-Aqueous Solution Interface. *Langmuir* **2006**, *22*, 4668−4673.
(12) Sung, J.; Zhang, L.; Tian, C.; Shen, Y. R.; Waychunas, G. A. Effect of pH on the Water/α-Al_2O_3 ($1\bar{1}02$) Interface Structure Studied by Sum-Frequency Vibrational Spectroscopy. *J. Phys. Chem. C* **2011**, *115*, 13887−13893.
(13) Al-Abadleh, H. A.; Grassian, V. H. FT-IR Study of Water Adsorption on Aluminum Oxide Surfaces. *Langmuir* **2003**, *19*, 341−347.
(14) Hasegawa, T.; Nishijo, J.; Imae, T.; Huo, Q.; Leblanc, R. M. Selective Observation of Boundary Water near a Solid/Water Interface by Variable-Angle Polarization Specific Attenuated Total Reflection Infrared Spectroscopy and Principal-Component Analysis. *J. Phys. Chem. B* **2001**, *105*, 12056−12060.
(15) Argyris, D.; Ho, T.; Cole, D. R.; Striolo, A. Molecular Dynamics Studies of Interfacial Water at the Alumina Surface. *J. Phys. Chem. C* **2011**, *115*, 2038−2046.
(16) Senapati, S.; Chandra, A. Dielectric Constant of Water Confined in a Nanocavity. *J. Phys. Chem. B* **2001**, *105*, 5106−5109.
(17) Sakuma, H.; Otsuki, K.; Kurihara, K. Viscosity and Lubricity of Aqueous NaCl Solution Confined between Mica Surfaces Studied by Shear Resonance Measurement. *Phys. Rev. Lett.* **2006**, *96*, 046104:1−4.
(18) Fenter, P.; Sturchio, N. C. Mineral-Water Interfacial Structures Revealed by Synchrotron X-ray Scattering. *Prog. Surf. Sci.* **2005**, *77*, 171−258.
(19) Harrick, N. J. *Internal Reflection Spectroscopy*; Harrick Scientific Corporation: New York, 1987.
(20) Seki, M.; Kobayashi, K.; Nakahara, J. Optical Spectra of Hexagonal Ice. *J. Phys. Soc. Jpn.* **1981**, *50*, 2643−2648.
(21) Shibaguchi, T.; Onuki, H.; Onaka, R. Electronic Structures of Water and Ice. *J. Phys. Soc. Jpn.* **1977**, *42*, 152−158.

DOI: 10.1021/acs.jpclett.5b00190
J. Phys. Chem. Lett. 2015, 6, 1022−1026

(22) Watanabe, K.; Zelikoff, M.; Force, A.; Command, D.; Leifson, S. W.; Henning, H. J.; Rathenau, G.; Hopfield, J. J.; Wilkinson, P. G.; Johnston, H. L.; Preston, W. M. Absorption Coefficients of Water Vapor in the Vacuum Ultraviolet. *J. Opt. Soc. Am.* **1953**, *43*, 753−755.
(23) Herzberg, G. *Molecular Spectra and Molecular Structure III. Electronic Spectra and Electronic Structure of Polyatomic Molecule*; D. Van Nostrand Company, Inc.: Princeton, NJ, 1966.
(24) Yabushita, A.; Hashikawa, Y.; Ikeda, A.; Kawasaki, M.; Tachikawa, H. Hydrogen Atom Formation from the Photodissociation of Water Ice at 193 nm. *J. Chem. Phys.* **2004**, *120*, 5463−5468.
(25) Minton, A. P. Far-Ultraviolet Spectrum of Ice. *J. Phys. Chem.* **1971**, *75*, 1162−1164.
(26) Lützenkirchen, J.; Zimmermann, R.; Preocanin, T.; Filby, A.; Kupcik, T.; Küttner, D.; Abdelmonem, A.; Schild, D.; Rabung, T.; Plaschke, M.; et al. An Attempt to Explain Bimodal Behaviour of the Sapphire c-Plane Electrolyte Interface. *Adv. Colloid Interface Sci.* **2010**, *157*, 61−74.
(27) Salmeron, M.; Bluhm, H.; Tatarkhanov, M.; Ketteler, G.; Shimizu, T. K.; Mugarza, A.; Deng, X.; Herranz, T.; Yamamoto, S.; Nilsson, A. Water Growth on Metals and Oxides: Binding, Dissociation and Role of Hydroxyl Groups. *Faraday Discuss.* **2009**, *141*, 221−229 (discussion 309−346).
(28) Wang, C.; Lu, H.; Wang, Z.; Xiu, P.; Zhou, B.; Zuo, G.; Wan, R.; Hu, J.; Fang, H. Stable Liquid Water Droplet on a Water Monolayer Formed at Room Temperature on Ionic Model Substrates. *Phys. Rev. Lett.* **2009**, *103*, 13708:1−4.
(29) Chipman, D. M. Excited Electronic States of Small Water Clusters. *J. Chem. Phys.* **2005**, *122*, 44111:1−10.
(30) Grigera, J. R. An Effective Pair Potential for Heavy Water. *J. Chem. Phys.* **2001**, *114*, 8064−8067.
(31) Harada, Y.; Tokushima, T.; Horikawa, Y.; Takahashi, O.; Niwa, H.; Kobayashi, M.; Oshima, M.; Senba, Y.; Ohashi, H.; Wikfeldt, K. T.; et al. Selective Probing of the OH or OD Stretch Vibration in Liquid Water Using Resonant Inelastic Soft-X-ray Scattering. *Phys. Rev. Lett.* **2013**, *111*, 193001:1−5.
(32) Hummer, G.; Garde, S.; Garcýìa, A. E.; Pratt, L. R. New Perspectives on Hydrophobic Effects. *Chem. Phys.* **2000**, *258*, 349−370.
(33) Rodnikova, M. N.; Chumaevskii, N. A. Three-Dimensional Net of Hydrogen Bonds in Liquids and Solutions. *J. Struct. Chem.* **2006**, *47*, S151−S158.

DOI: 10.1021/acs.jpclett.5b00190
J. Phys. Chem. Lett. 2015, 6, 1022−1026